Interpretation of some properties of A-V conduction with the help of analog simulation

Robert M. Heethaar[1,2], Jan J. Denier van der Gon[2] and Frits L. Meijler[1]

[1]*Department of Cardiology, University Hospital, and* [2]*Department of Medical Physics, University of Utrecht, Utrecht, The Netherlands*

HEETHAAR, R.M., DENIER VAN DER GON, J.J. and MEIJLER, F.L. (1973): Interpretation of some properties of A-V conduction with the help of analog simulation. *Europ. J. Cardiol., 1/1*, 87–93.

For a better understanding of the phenomenological characteristics of A-V nodal conduction the impulse propagation through a transmission line consisting of units obeying the Bonhoeffer-Van der Poll equations was studied. It appears that impulse propagation through such a transmission line shows similarity with A-V nodal conduction.

Bonhoeffer-Van der Poll model; impulse transmission line

Introduction

In this research we have attempted to improve our understanding of a number of A-V nodal conductive properties by means of an analog model. In a crude simplification the A-V node can be considered as a series of coupled excitable cells. If one cell is excited, it excites in turn an adjacent cell and so on, the whole chain behaving as an impulse transmission line. It was thought to be of interest to know if a transmission line composed of excitable artificial cells, having typical electrophysiological properties, demonstrates the main conductive properties of the A-V node, at least qualitatively. If so, properties of the A-V nodal cells may possible be related to general membrane properties of excitable cells, which have many features in common and as far as they differ they do so mainly in detail [1]. Also suggestions for future live experiments may be obtained in this way.

For a preliminary scanning of this field the approach of Nagumo et al. [9] has been followed. They described a transmission line which basically exists of units obeying the Bonhoeffer-Van der Poll equations. Although the simplification has its drawbacks we found that this model and the A-V node are already more or less similar with respect to a number of conductive properties.

Methods

Equations describing the excitation of axons in the case of spatially uniformly excited membranes have been given by Hodgkin and Huxley [5]. FitzHugh [2] demonstrated that a projection of the four dimensional Hodgkin-Huxley phase space onto a plane shows similar diagrams of nerve excitation as were produced by the Bonhoeffer-Van der Poll model [2] based on a set of nonlinear differential equations mentioned below.

In principle this projection consists of combining the parameters V and m of the Hodgkin-Huxley equations into $V-36m$, and combining the n and h parameters into $0.5(n-h)$, where V is the membrane voltage,

m the sodium activation, h the sodium inactivation and n is the potassium activation. The Bonhoeffer-Van der Poll equations are given by

$$J = \frac{1}{c} \frac{du}{dt} - w - (u - \tfrac{1}{3}u^3)$$

$$c \frac{dw}{dt} + bw = a - u \tag{1}$$

The variable u shows properties of excitability, whereas w represents accomodation and refractoriness and changes relatively slowly. J corresponds to membrane current density. The constants a, b and c must satisfy the relations:

$$0 < b < 1, \quad b < c^2 \quad \text{and} \quad 1 - \tfrac{2}{3}b < a < 1$$

The equations belong to a class of equations which describe excitable-oscillatory systems. Nagumo [9] has proceeded as follows: for the electronic circuit in Figure 1 where T is a tunnel diode the following relations are valid:

$$j = C \frac{dv}{d\tau} - i - f(e)$$

$$L \frac{di}{d\tau} + Ri = -v = e - E_0 \tag{2}$$

where f(e) is the voltage-current characteristic of the tunnel diode. To a first approximation this function may be written as:

$$f(e) = i_0 - \frac{1}{\rho} \left[(e - e_0) - \frac{(e - e_0)^3}{3K^2} \right] \quad (\rho > 0, K > 0)$$

where ρ, i_0 and K are constants. For $e = e_0$ f(e) equals i_0 and has a turning point and the differential resis-
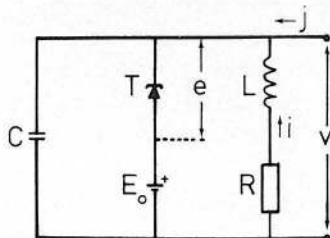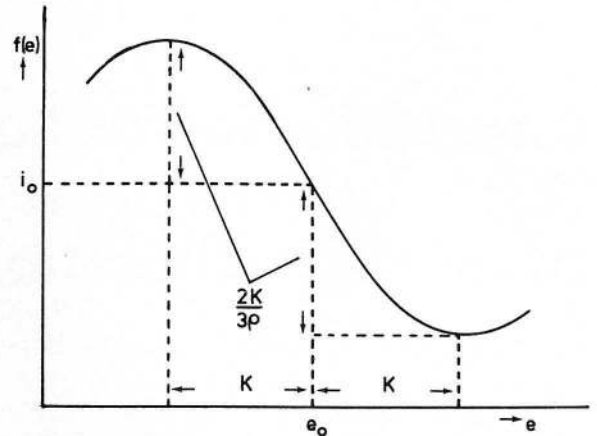

Fig. 2. Approximation of the voltage-current characteristic of the tunnel diode.

tance of the diode is $-\rho$. In figure 2 f(e) is plotted versus e. By introducing new variables:

$$t = \frac{\tau}{\sqrt{LC}}, \quad u = \frac{v + (e_0 - E_0)}{K}, \quad w = \frac{\rho}{K}(i + i_0), \quad J = \frac{\rho}{K}j,$$

$$b = \frac{R}{\rho}, \quad c = \frac{1}{\rho}\sqrt{\frac{L}{C}} \quad \text{and} \quad a = \frac{Ri_0 + (e_0 - E_0)}{K}$$

it can be shown that (1) reduces to (2). The conditions for a, b and c result in:

$$\rho > R, \quad \frac{L}{R} > \rho C,$$

$$Ri_0 + (e_0 - K) < E_0 < R\left(i_0 + \frac{2K}{3\rho}\right) + (e_0 - K)$$

By coupling the units through resistances r an impulse transmission line is created (see Fig. 3A). It can be shown that the circuit of Figure 3B has equal properties with regard to impulse transmission as the circuit of Figure 3A. For practical reasons the circuit of Figure 3B is chosen for the experiments. As a result of the choice of the parameter values a timescaling has been introduced and the simulation results are not on a real time base. Up till now we have followed the train of thought of Nagumo. Below we give our experiments concerning the transmission delays as a function of stimulation intervals, whereas Nagumo [9] has dealt with the attenuation and distortion properties of the impulse transmission line.

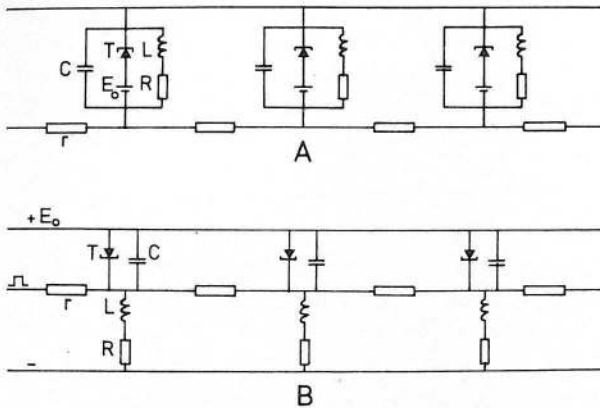Fig. 1. Electronic circuit, simulating the Bonhoeffer-Van der Poll model.

Fig. 3. Impulse transmission line, consisting of several units of Fig. 2, coupled by resistances r (A). In B an impulse transmission line is given having the same properties as the circuit in A (R=40 ohm, $10 < r < 470$ ohm, L=5 mH and C=0.47 μF).

Results

1. Fixed rates

First the model has been stimulated with constant stimulation rates. It was found that the delays between the stimulation impulses and upstrokes of the 'evoked' action potentials increased at decreasing stimulation intervals. The delays at the 21st unit ver-
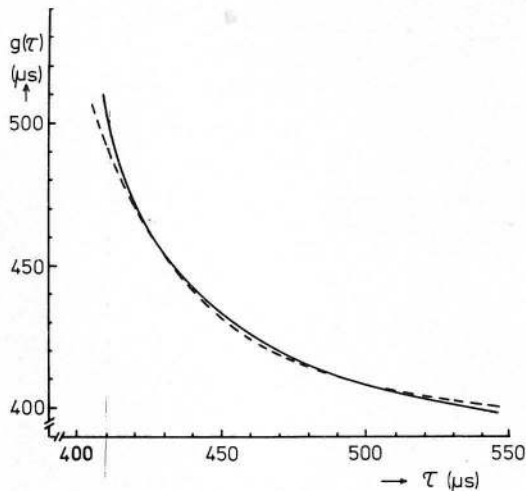

Fig. 4. Steady state relation between total conduction delay and stimulation interval (continuous line). Results were obtained from an impulse transmission line shown in Fig. 3B using 21 units. The dashed line shows a plot of the funtion $g(\tau) = A \exp(-\alpha\tau) + C$. (A = 5.95 10^6, $1/\alpha$ = 37.3 μsec and C = 400 μsec).
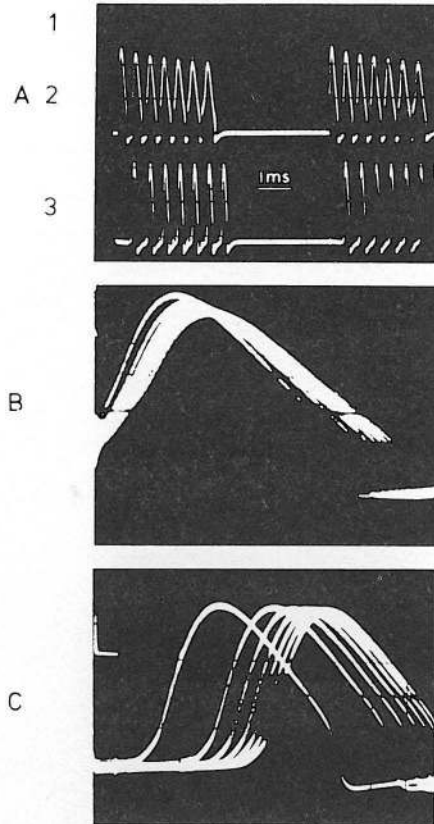

Fig. 5. Oscilloscope recordings of the responses of the first (A second trace and B) and the last unit (A third trace and C) after a frequency step. The first trace of A shows the stimulation pulses. B, resp. C is a triggered superposition of A2, resp. A3.

sus the stimulation intervals have been plotted in Figure 4. This result can be compared with the steady-state relation between conduction time and stimulation interval for the A-V node [4, 6].

2. Frequency steps

a. Another rather essential property of the A-V node, namely its gradual adaptation to frequency changes, can also be demonstrated with the analog model. This is shown in Figures 5 and 6. In Figure 5A the stimulation impulses are shown together with the responses of the first cell and the last cell, respectively. In Figure 5B a superposition of the responses of the first cell is given. In Figure 5C the responses of
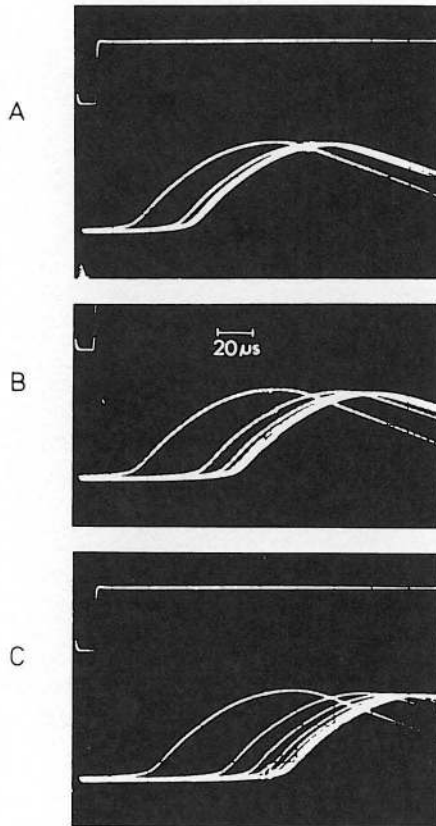
Fig. 6. Oscilloscope recordings of the responses of the last cell, showing increasing conduction time after a frequency step from 4.5 msec to 440 μsec (A), 420 μsec (B) and 415 μ sec (C). The scope is triggered at a pulse 330 μsec after the stimulation pulses (upper traces in A, B and C).

tion of a whole chain it cannot be concluded that each single cell also shows this property. It can be shown that a transmission line consisting of units of which the transmission delay is determined solely by the last stimulus interval will show gradual adaptation effects more or less similar to the adaptation effect found in the A-V node. This has been proved theoretically for transmission lines consisting of different numbers of cells. For simplicity the train of thought is given below for a transmission line of two elements for a frequency step from τ_0 to τ_1 (see Fig. 7) whereas the transmission delay of each cell is considered to be given by the function $g(\tau)$ from Figure 4. In the steady state, with stimulation interval τ_0 the delay of each cell is g_0, as indicated at the first two intervals of Figure 7 (A). After the first impulse after the frequency step the situation as indicated by B in Figure 7 is created. After the second impulse the situation C is achieved. The total delays after the first, respectively second impulse after the frequency step are $g_1 + g_2$, respectively $2g_1$. From this it can be seen that a transmission line consisting of elements of which the delay depends only on the preceding stimulation interval already shows gradual adaptation properties.
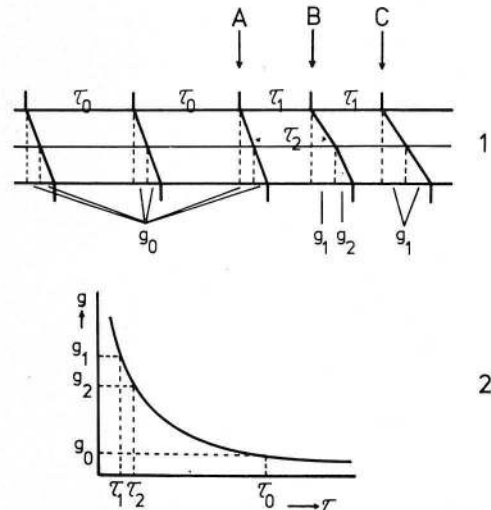
In Figure 8 the normalized adaptations to a fre-

the last cell are superimposed. In Figure 5B the oscilloscope is triggered by the stimulation pulses, in Figure 5C by a pulse with a constant delay after the stimulation pulses. This figure shows that the total delay increases gradually. Also in Figure 6 recordings are shown of the 'action potentials' of the last cell. It can be concluded that the adaptation to frequency changes tends to the adaptation properties found for A-V nodal tissue [3, 4], i.e. the number of beats during the adaptation to a new rhythm changes relatively more than the duration of the adaptation.

 b. Gradual adaptation of a single cell to frequency changes will result in gradual adaptation of the whole transmission line. However, from the gradual adapta-

Fig. 7. Gradual adaptation of conduction time g for two cells after a frequency step in stimulation interval from τ_0 to τ_1 (1) derived from the steady state relation (2) between conduction time and stimulation interval.
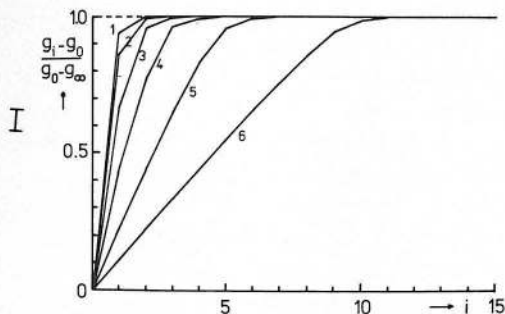
Fig. 8. Plots of computed normalized adaptation of delay after a step from 400 to 500 μsec of transmission lines consisting of 10 (1), 20 (2), 40, 80, 160, resp. 230 (6) units, g_0, resp. g_∞ indicate the steady state conduction times at stimulation intervals of 400, resp. 500 μsec.

quency step from 400 to 500 μsec of transmission lines consisting of different numbes of cells of which the conduction delay is given by $g(\tau)/21$ have been plotted. The function g has been taken from Figure 4. It can be seen that the adaptation takes more time for transmission lines consisting of more elements.
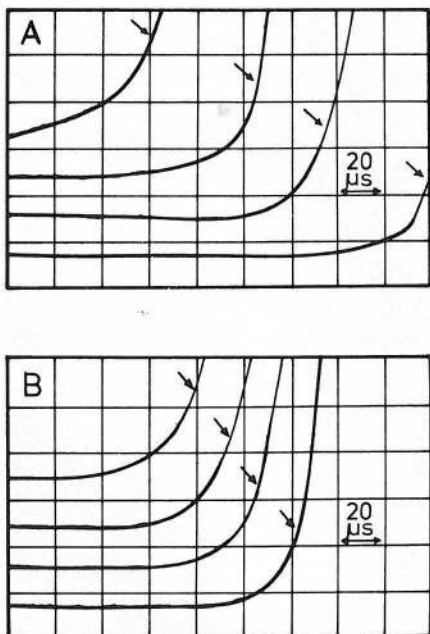

Fig. 9. Excitation moments of four successive units (cells 15, 16, 17, 18) of the transmission line in case the coupling resistances are 470, resp. 20 ohm (B). The arrows indicate the thresholds of the several units.

3. Cell coupling

In the analog model each cell is triggered by the previous one. In Figure 9A the moments of excitation of four successive cells in the chain and the way they reach their thresholds are shown. In this experiment where the coupling resistances r are 470 ohm, the influence in the nonactive state of a cell upon the adjacent one is negligible, as the potential of the adjacent cell only starts to rise after the foregoing cell has passed its threshold. When the coupling resistances were reduced to 20 ohm this influence was still weak but not negligible. This is shown in Figure 9B.

4. Blocking of impulses

Also blocking phenomena could be demonstrated. This is shown in Figure 10 (A-H). In each part of the
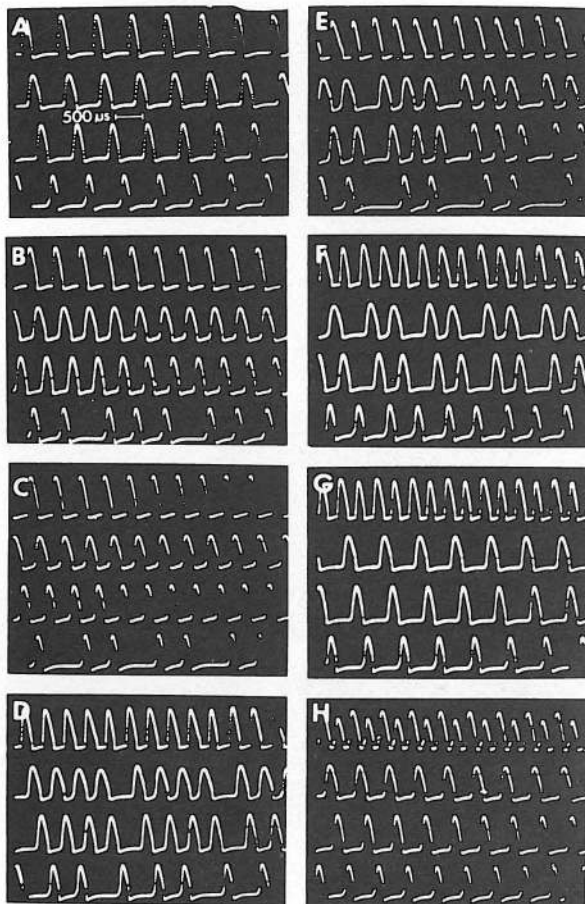

Fig. 10. Responses of four cells from the transmission line in different situations of constant stimulation.

figure four recordings are shown, i.e. the responses of the second, the seventh, the fifteenth and the last (21st) cell, respectively. In A, all stimuli were conducted through the analog model. In B, blocking of impulses occurred between the fifteenth and the last cell (4:3 block). Increase of stimulation frequency causes an increase in blocked pulses in the last part of the transmission line (3:2 block) (C). A further increase of stimulation frequency can cause several types of blocking of impulses (Figure 10 D,E,F,G,H).

5. Dual pathways

Up till now only one-dimensional models have been considered here. We thought it of interest to study the behavior of a chain with two parallel pathways of e.g. different lengths [7, 8]. Apart from the concept of longitudinal dissociation in the A-V node the cells in a pathway in the A-V node will not only be ranged after each other. In Figure 11A the chain used is given schematically. In Figure 11B the response to stimuli is shown for the first cell (first trace), for the last cell in the α-pathway (α_1), for the last cell in the β-pathway (β_1) and for the cell where

the α- and the β-pathway meet each other ($\alpha\beta$). The coupling resistances between α_1-$\alpha\beta$ and β_1-$\alpha\beta$ are chosen so that neither α_1 nor β_1 alone can excite $\alpha\beta$. The activations of both cells are necessary to activate $\alpha\beta$. Because the α-pathway is shorter than the other, the α_1 response reaches $\alpha\beta$ earlier than the β_1 response. In the fourth trace of Figure 11B a local response due to the α_1 response is shown. After the β_1 response the unit $\alpha\beta$ is excited. Increase in stimulus frequency causes slightly increased conduction times along the α- and β-pathways and may eventually cause blocking of impulses. The result of such a frequency change is shown in Figure 11C. Now, two local activations due to the α_1 and β_1 responses can be seen.

Discussion

For reasons mentioned in the introduction it is of interest to compare the conductive properties of the impulse transmission line described above with the properties of the A-V node [3, 4]. First attention has been focussed upon the relationship between conduction time and stimulation rate. The general trend in both cases is rather similar. As a next point, in agreement with the phenomenological results found for the A-V node, gradual adaptation of the conduction time after a step in stimulation rate is also found in the transmission line. Such an adaptation could be detected weakly in a single unit. However, a transmission line consisting of units of which the transmission delay is determined solely by the last stimulus interval already shows adaptation effects more or less similar to the adaptation effect found in the real A-V node. From these results it may be concluded that the A-V node, although it does not adapt itself instantaneously to changes in stimulation rate does not necessarily consist of elements which show gradual adaptation properties. Another property of the A-V node is that impulses may be blocked inside the node. Such a property could indeed be shown in the single pathway transmission line. Blocking is found at different levels. However, it should be stressed that these effects are allied to inhomogenities in the transmission line. It may be that the behavior of the line becomes more complicated and less predictable when via the coupling resistances not only the directly preceeding unit influences a subsequent one, but that a
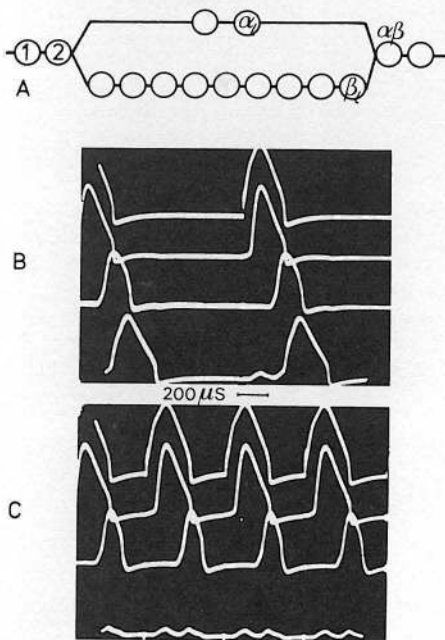

Fig. 11. Responses of the cells 1, α_1, β_1, resp. $\alpha\beta$ of the transmission line given in A for different stimulation intervals.

cell is influenced by other units as well. In the afore-mentioned transmission line such effects were very weak and their contribution to the overall properties of the line are negligible.

Total blocking of impulses could be demonstrated in a transmission line with two pathways. In the range of low stimulation frequences this was not possible for a transmission line consisting of a single pathway. Also the phenomenon 'concealed conduction' can be simulated by coupled differential equations belonging to the same class as mentioned above [11]. From the aforementioned results it appears that a transmission line consisting of simple excitable units may show already in a qualitative way some properties as found for the A-V conduction system in situ. For establishing more quantitative relations between properties of A-V nodal cells and their coupling to conduction properties of the A-V node, the elements used here are not well enough representative for A-V nodal cells. Therefore it is felt worthwhile to continue this research by considering also transmission lines consisting of units based on the Hodgkin-Huxley equations modified by Noble and coupled in a more realistic way. Up till now the results demonstrate that:

1. with the model in vivo situations can be simulated,
2. such simulation may contribute to the understanding of A-V nodal conduction properties.

References

[1] Cole, K.S. (1968): *Membranes, Ions and Impulses*. University of California Press, Berkeley and Los Angeles, Calif.

[2] FitzHugh, R. (1961): Impulses and physiological states in theoretical models of nerve membrane. *Biophys. J., 1*, 445.

[3] Heethaar, R.M., Denier van der Gon, J.J. and Meijler, F.L. (1973a): A mathematical model of A-V conduction in the rat heart. *Cardiovasc. Res., 7*, 105.

[4] Heethaar, R.M., De Vos Burchart, R.M., Denier van der Gon, J.J. and Meijler, F.L. (1973b): A mathematical model of A-V conduction in the rat heart II. *Cardiovasc. Res.*, in press.

[5] Hodgkin, A.L. and Huxley, A.F. (1952): A quantitative description of membrane current and its application to conduction and excitation in nerve. *J. Physiol., 117*, 500.

[6] Merideth, J., Mendez, C., Mueller, W.J. and Moe, G.K. (1968): Electrical excitability of atrioventricular nodal cells. *Circulat. Res., 23*, 69.

[7] Mendez, C. and Moe, G.K. (1966): Demonstration of a dual A-V nodal conduction system in the isolated rabbit heart. *Circulat. Res., 19*, 378.

[8] Moe, G.K., Preston, J.B. and Burlington, H. (1956): Physiologic evidence for a dual A-V transmission system. *Circulat. Res. 4*, 357.

[9] Nagumo, J., Arimoto, S. and Yoshizawa, S. (1962): An active pulse transmission line simulating nerve axon. *Proc. Inst. Radio Engrs, 50*, 2061.

[10] Noble, D. (1962): A modification of the Hodgkin–Huxley equations applicable to Purkinje fibre action and pacemaker potentials. *J. Physiol., 160*, 317.

[11] Roberge, F.A. (1969): Simulation of the phenomenon concealed conduction. *Comput. biomed. Res., 2*, 362.